Anal. Chem. **2002,** *74,* 4343−4352

Rapid Screening of Aqueous Chemical Warfare Agent Degradation Products: Ambient Pressure Ion Mobility Mass Spectrometry

Wes E. Steiner, Brian H. Clowers, Laura M. Matz, William F. Siems, and Herbert H. Hill, Jr.*

Department of Chemistry, Washington State University, Pullman, Washington 99164-4630

The use of electrospray ionization ambient pressure ion mobility spectrometry with an orthogonal reflector time-of-flight mass spectrometer to analyze chemical warfare (CW) degradation products from aqueous environmental samples has been demonstrated. Certified reference materials of analytical standards for the detection of Schedule 1, 2, or 3 toxic chemicals or their precursors as defined by the chemical warfare convention treaty verification were used in this study. A combination of six G/V-type nerve and four S-type vesicant related CW agent degradation products were separated with baseline resolution by this instrumental technique. Analytical figures of merit for each CW degradation product were determined. In some cases, reduced mobility constants (K_0) have been reported for the first time. Linear response ranges for the selected CW degradation products were found to be generally ∼2 orders of magnitude, where the overall dynamic response ranges were found to extend to 4 orders of magnitude. Limits of detection for five of the nine chemical products tested were found to be less than 1 ppm. To demonstrate the potential of this instrumental method with complex mixtures, four CW degradation products were separated and detected from a spiked Palouse River water sample in less than 1 min. Finally, a homologous series of *n*-alkylamines were used as baseline reference standards, producing a mobility/mass trend line to which the CW degradation products could be compared. Comparison of these products in this manner is expected to reduce the number of false positive/negative responses.

Since their introduction—and throughout their ongoing development—the rapid detection of chemical warfare (CW) agents and their corresponding degradation products in environmental samples has been an important area of research. Implementation of the Chemical Weapons Conventions (CWC) banning the development, production, acquisition, retention, and direct or indirect transfer of chemical weapons has mandated the destruction of all chemical weapons held in reserve.[1] To comply with the mandates established by this convention, it is necessary to develop reliable methods of detection for CW agents and their related products. In addition to treaty verification, ensuring the integrity of aqueous resources that are relied upon by both military and civilian populations is a top priority.[2] Thus, there is a need for the development of a rapid analytical method for the characterization of a broad spectrum of CW agents and other toxic compounds in aqueous samples.

Chemical warfare agents are historically classified as either nerve or vesicant agents. Under normal environmental conditions, CW agents are considered extremely reactive and possess varying degrees of environmental lifetimes depending on the method of dissemination.[3] The nerve agents Tabun (GA), Sarin (GB), Soman (GD), and VX all disrupt neurological regulation within biological systems through the inhibition of acetyl cholinesterase.[4] The vesicant agents—also known as bifunction alkylating agents—sulfur mustard gas (HD), lewisite (L), nitrogen mustard gas (HN), and phosgene−oxime (CX) are the agents typically responsible for blistering action.[5] Environmental neutralization of CW agents typically involves the degradation of the parent compound to yield various hydrolysis products.[6−8] The G-type nerve agents—which include GA, GB, and GD—rapidly hydrolyze to form various alkyl phosphonic acids. Whereas, V-type or VX nerve agents degrade to form alkyl phosphonic acids, phosphonothioic acids, along with 2-(diisopropylamino)ethanethiol (DESH), 2-(diisopropylamino)-ethanol (DIPAE), 2-(diethylamino)ethanol (DEAE), and *S*-2-(diisopropylamino)ethylmethylphosphonic acid (EA2192). The

* To whom correspondence should be addressed. Tel: (509) 335-5648. Fax: (509) 335-8867. E-mail: hhhill@wsu.edu.

(1) *Chemical Weapons Convention (CWC) bans the development, production, acquisition,* stockpiling, *and use of Chemical Weapons and on their destruction*. Washington D.C. United States Bureau of Arms Control and Disarmament Agency, Entered into force April 29, 1997.

(2) *Guidelines for Chemical Warfare Agents in Military Drinking Water. Washington D.C.* Subcommittee on Guidelines for Military Field Drinking-Water Quality, 1995.

(3) Bizzigotti, G. *Biological and Chemical Warfare Agent Dissemination*; Mitretek Systems, 2001; pp 54−58.

(4) Burgen, A. S. V.; Hobbiger, S. *Br. J. Pharmacol. Chemother.* **1951**, *6*, 593−605. Koelle, G. B.; Ballantyne, B.; Marrs, T. C. *Pharmacology and toxicology of organophosphates*; Butterworth-Heinemann: Oxford, 1992; pp 35−39. Compton, J. A. F. *Military Chemical and Biological Agents: Chemical and Toxicological Properties*; The Telford Press: Caldwell, NJ, 1987. Grob, D.; Hervey, A. M. *Am. J. Med.* **1953**, *14*, 52−63. Grob, D. *Arch. Intern. Med.* **1956**, *98*, 221−239. Grob, D.; Harvey, A. M. *J. Clin. Invest.* **1958**, *37*, 350−368.

(5) Fox, M.; Scott, D. *Mutat. Res.* **1980**, *75*, 131−168.

(6) Kingery, A. F.; Allen, H. E. *Toxicol. Environ. Chem.* **1995**, *47*, 155−184.

(7) Vasil'ev, I. A.; Shvyryaev, B. V.; Liberman, B. M.; Sheluchenko, V. V.; Petrunin, V. A.; Gorskii, V. G. *Mendeleev Chem. J.* **1996**, *39* (4), 3−10. Yang, Y. C.; Bake, J. A.; Ward, J. R. *Chem. Rev.* **1992**, *92*, 1729−1743. Yang, Y. C. *Acc. Chem. Res.* **1999**, *32*, 109−115. Wagner, G. W.; Yang, Y. C. *Ind. Eng. Chem. Res.* **2002**, *41* (8), 1925−1928.

(8) Cheicante, R. L.; Stuff, J. R.; Durst, H. D. *J. Capillary Electrophor.* **1995**, *4*, 157−163.

10.1021/ac025687f CCC: $22.00
Published on Web 07/31/2002

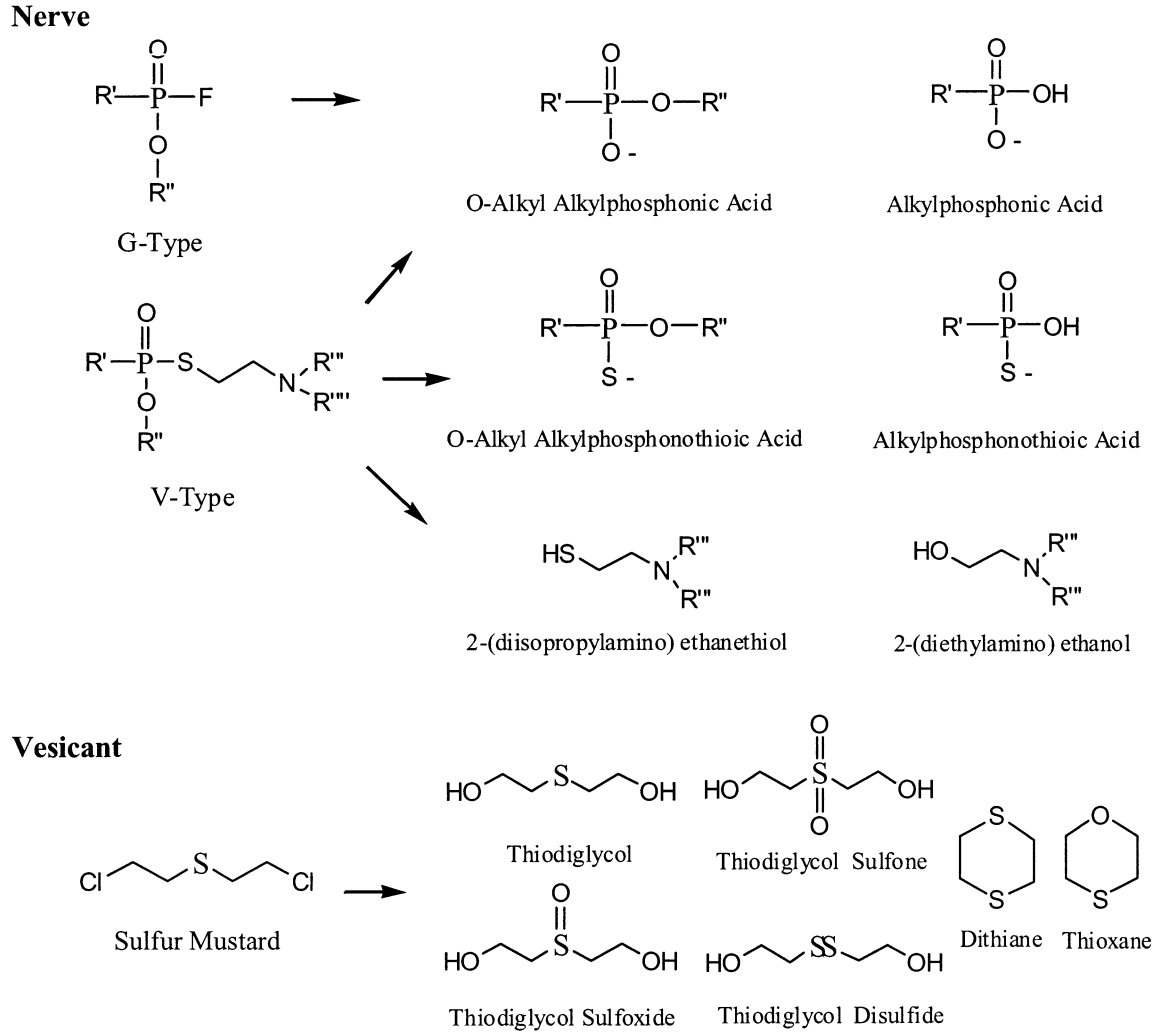

Figure 1. Common degradation pathways for nerve and vesicant CW agents in water. R′ = CH_3, CH_3CH_2, $CH_3CH_2CH_2$, or $(CH3)_2CH_2$; R″ = =C10 as well as cycloalkyls; R‴ = H or =C10 including cycloalkyls; and R⁗ = CH_3, CH_3CH_2, $CH_3CH_2CH_2$, or $(CH3)_2CH_2$.

common sulfur- and arsenic-containing vesicants HD and L typically degrade to produce thiodiglycol (TDG), thiodiglycol sulfone (TDGO2), thiodiglycol sulfoxide (TDGO), 2-(hydroxyethyl) ethyl sulfide (HEES), bis(2-hydroxyethyl) disulfide (BHEES), 1,4-dithiane, 1,4-thioxane, 2-chlorovinylarsonous acid (CVAA), and 2-chlorovinylarsonous oxide (CVAO), respectively. A brief decomposition scheme is shown in Figure 1. A more comprehensive decomposition scheme for the two classes of CW agents can be found in ref 8. The degradation products found in Figure 1 tend to exhibit a higher degree of stability and persistence in the environment than their corresponding parent agents.[6] Direct detection of the CW degradation products provides a convenient and indirect detection method for CW agents.

The highly polar and nonvolatile degradation products of CW agents readily dissolve in aqueous environments, making them unsuitable for use in common separation schemes employing nonaqueous media such as gas chromatography (GC). Separation schemes employing aqueous mobile phases such as high-performance liquid chromatography (HPLC) are well suited for CW degradation product separation. However, analyte detection using traditional HPLC detectors such as ultraviolet (UV)/fluorescence (F) absorption/emission is difficult as most CW agents and their degradation products lack prominent chromophores. For these reasons (lack of chromophores or volatility), analysis of CW degradation products using HPLC and GC techniques has historically required some type of chemical derivatization. Chemical modifications enable these compounds to be detected by either HPLC/fluorescence[9] or gas chromatographic separation followed by mass spectrometry (GC/MS).[10] Derivatization for either method requires extensive sample preparation and is comparatively expensive and time-consuming. In addition to derivatization schemes, a number of sensitive detection methods exist for the analysis of aqueous samples. However, these too are limited in their scope of applicability. Ion chromatography with conductivity detection[11] has proven to be an effective method for the detection of analytes in aqueous samples but is limited by its susceptibility to interferences and requires extensive sample cleanup for the analysis of complex environmental samples. Mass spectrometry employing various nebulizing ionization techniques[12] has adequate detection limits

(9) Roach, M. C.; Unger, L. W.; Zare, R. N.; Reimer, L. M.; Pumpliano, J. W.; Frost, J. W. *Anal Chem.* **1987**, *59*, 1056−1059. Garfield, P. J.; Pagotto, J. G.; Miller R. K. *J. Chromatogr.* **1989**, *475*, 261.

(10) Tornes, J. A.; Johnson, B. A. *J. Chromatogr.* **1989**, *467*, 129−138. Kientz, C. E. *J. Chromatogr., A* **1998**, *814*, 1. Kingery, A. F.; Allen H. E. *Anal. Chem.* **1994**, *66*, 155.

(11) Bossle, P. C.; Reutter, D. J.; Sarver, E. W. *J. Chromatogr.* **1987**, *407*, 399.

with unambiguous peak detection but is limited in some cases by its durability requirement of clean samples.

Other analytical methods that have been proposed for the detection of CW agents in aqueous samples include the following: (1) Bioaccumulation followed by GC/MS,[13] which provided excellent detection limits, but is time-consuming and expensive; (2) capillary zone electrophoresis (CZE) with UV detection,[8] but as previously stated, many CW degradation products do not absorb UV light. In addition to problems associated with detection, CZE required four separate analyses to separate and detect all of the compounds investigated, making the technique tedious and resource intensive; and (3) ion mobility spectrometry (IMS), which has been used for the trace analysis of vapor-phase compounds such as explosives, drugs, and CW agents.[14]

Developments in electrospray ionization (ESI) by our laboratory have enabled the direct determination of nonvolatile compounds from liquid samples by ambient pressure (AP) IMS.[15] While it is a sensitive detection method, low resolving power has limited IMS as a separation method for complex mixtures. Thus, chromatographic separations prior to IMS for the analysis of complex mixtures has been required. The development of an ambient pressure high-resolution ion mobility spectrometer[16] with resolving powers similar to or better than typical HPLC separations has allowed the technique to function as a stand-alone separation device. By eliminating chromatographic separations and relying solely upon the separation capabilities of high-resolution IMS, it is possible to separate and detect analytes in less than 1 s. This is the primary advantage of ESI-IMS over traditional chromatographic methods (HPLC and GC), which require several minutes to hours to separate analytes.

Preliminary work in coupling ESI-IMS with MS for CW degradation product analysis demonstrated the potential for the characterization of aqueous-phase samples by two-dimensional ion mobility mass spectrometry (IMMS). These first IMMS investigations employed common quadrupole mass spectrometers.[17] However, this arrangement was found to be relatively slow because of the need to scan m/z values sequentially in the quadrupole mass filter to obtain 2-D spectra. To address this problem, our laboratory has interfaced an ambient pressure IMS to a time-of-flight (TOF) MS, which is capable of acquiring complete mass spectra for each mobility peak. This comparatively rapid method of 2-D data acquisition makes this IMMS hybrid instrument suitable for the rapid detection of CW degradation products.[18]

This study explores the feasibility of using an electrospray ionization ambient pressure ion mobility spectrometer interfaced to an orthogonal reflector time-of-flight mass spectrometer (ESI/APIMS/TOFMS or IMMS) for the rapid detection of CW degradation products from aqueous sample matrixes. Several factors related to the detection of aqueous-phase CW degradation products that were investigated include the following: (1) scan time, (2) sensitivity, (3) limits of detection, (4) reproducibility, (5) trend-line referencing, and (6) matrix effects on sample identification.

EXPERIMENTAL SECTION

Chemicals and Solvents. The nine CW degradation products (1,4-dithiane, thiodiglycol, thiodiglycol sulfoxide, methylphosphonic acid, ethylmethylphosphonic acid, isopropylmethylphosphonic acid, cyclohexylmethylphosphonic acid, pinacoylmethylphosphonic acid, diisopropylmethylphosphonate) used were obtained from Cerilliant (Austin, TX) as 1 mg/mL certified reference materials (CRMs). These CRMs are used as analytical standard solutions for the detection of Schedule 1, 2, or 3 toxic chemicals or their precursors as stated in the CWC verification and related analysis annex.[1] These Schedules outline a list of prohibited and monitored chemicals for the purposes of implementing the CWC. Nine *n*-alkylamines (pentyl-, hexyl-, heptyl-, octyl-, nonyl-, decyl-, undecyl-, dodecyl-, and tridecylamine) were purchased from Sigma Aldrich Chemical Co. (St. Louis, MO) as puriss (99.5%) standards. Stock solutions for these CW degradation products and *n*-alkylamines were prepared in ESI solvent (47.5% water, 47.5% methanol, 5% acetic acid) at concentrations of 1000 ppm (1000 μg/mL), respectively. Further dilutions of these stock solutions with ESI solvent ranged from 10 ppb to 500 ppm (0.01−500 μg/mL), depending upon the experiment. The HPLC grade ESI solvents (water, methanol, acetic acid) were purchased from J. T. Baker (Phillipsburgh, NJ). The environmental water samples used in this study were collected from our laboratory drinking water supply and directly from the Palouse River in Pullman, WA. Both water samples were filtered through a 0.20-μm Nalgene filter (Sybron Corp., Rochester, NY) to prevent any unwanted particulate matter from entering the system. No further sample preparation was performed on either water samples.

Instrumentation. The IMMS instrument used in this study was constructed at Washington State University where the fundamental components (ESI source, APIMS drift tube, high-pressure interface, TOF m/z analyzer, and data acquisition system) were previously described in detail[18] and are shown in Figure 2. The operating parameters for each component are described below. As the operating principles and experimental procedures used in ion mobility spectrometry have been presented previously in detail,[19] only a short outline of the experimental sequence is provided. Desolvated ions from the electrospray process drifted through an APIMS tube under a weak uniform

(12) Wils, E. R. J.; Hulst, A. G. *J. Chromatogr.* **1988**, *454*, 261−272. Kostianen, R.; Bruins, A. P.; Hakkinen, V. M. A. *J. Chromatogr.* **1993**, *634*, 113−118. Borrett, V. T.; Mathews, R. J.; Colton, R.; Traeger, J. C. *Rapid Commun. Mass Spectrom.* **1996**, *10*, 114. Black, R. M.; Read, R. W. *J. Chromatogr.* **1997**, *759*, 79−92. D'Agostino, P. A.; Chenier, C. L.; Hancock, J. R. *J. Chromatogr., A* **2002**, *950*, 149−156. D'Agostino, P. A.; Hancock, J. R.; Provost, L. R. *J. Chromatogr., A* **2001**, *912*, 291−299. Read, R. W.; Black, R. M. *J. Chromatogr., A* **1999**, *862*, 169−177. D'Agostino, P. A.; Hancock, J. R.; Provost, L. R. *J. Chromatogr., A* **1999**, *840*, 289−294. Black, R. M.; Read, R. W. *J. Chromatogr., A* **1998**, *794*, 233−244.

(13) Ferrarlo, J. B.; Deleon, I. R.; Peuler, E. A. *Environ. Sci. Technol.* **1994**, *28*, 1893−1897.

(14) Eiceman, G. A.; Karpas, Z. *Ion Mobility Spectrometry*; CRC Press: Boca Raton, FL, 1994.

(15) Wittmer, D.; Chen, Y. H.; Luckenbill, B. K.; Hill, H. H., Jr. *Anal. Chem.* **1994**, *66*, 2348−2355. Shumate, C. B.; Hill, H. H. *Anal. Chem.* **1989**, *61*, 601.

(16) Wu, C.; Siems, W. F.; Asbury, G. R.; Hill, H. H., Jr. *Anal. Chem.* **1998**, *70*, 4929−4938. Dugourd, P. H.; Hudgins, R. R.; Clemmer, D. E.; Jarrold, M. F. *Rev. Sci. Instrum.* **1997**, *68*, 1122.

(17) Chen, Y. H.; Siems, W. F.; Hill, H. H., Jr. *Anal. Chim. Acta* **1996**, *334*, 75−84. Asbury, R. G.; Wu, C.; Siems, W. F.; Hill, H. H. *Anal. Chim. Acta* **2000**, *404*, 273−283. Karasek, F. W.; Hill, H. H.; Kim, S. H. *J. Chromatogr. Sci.* **1976**, *117*, 327. Hoaglund, C. S.; Valentine, S. J.; Clemmer, D. E. *Anal. Chem.* **1997**, *69*, 4156−4161. Purves, R. W.; Guevremont, R.; Day, S.; Pipich, C. W.; Matyjaszcayk, M. S. *Rev. Sci. Instrum.* **1998**, *69*, 4094.

(18) Steiner, W. E.; Clowers, B. H.; Fuhrer, K.; Gonin, M.; Matz, L. M.; Siems, W. F.; Schultz, A. J.; Hill, H. H. *Rapid Commun. Mass Spectrom.* **2001**, *15* (23), 2221−2226.

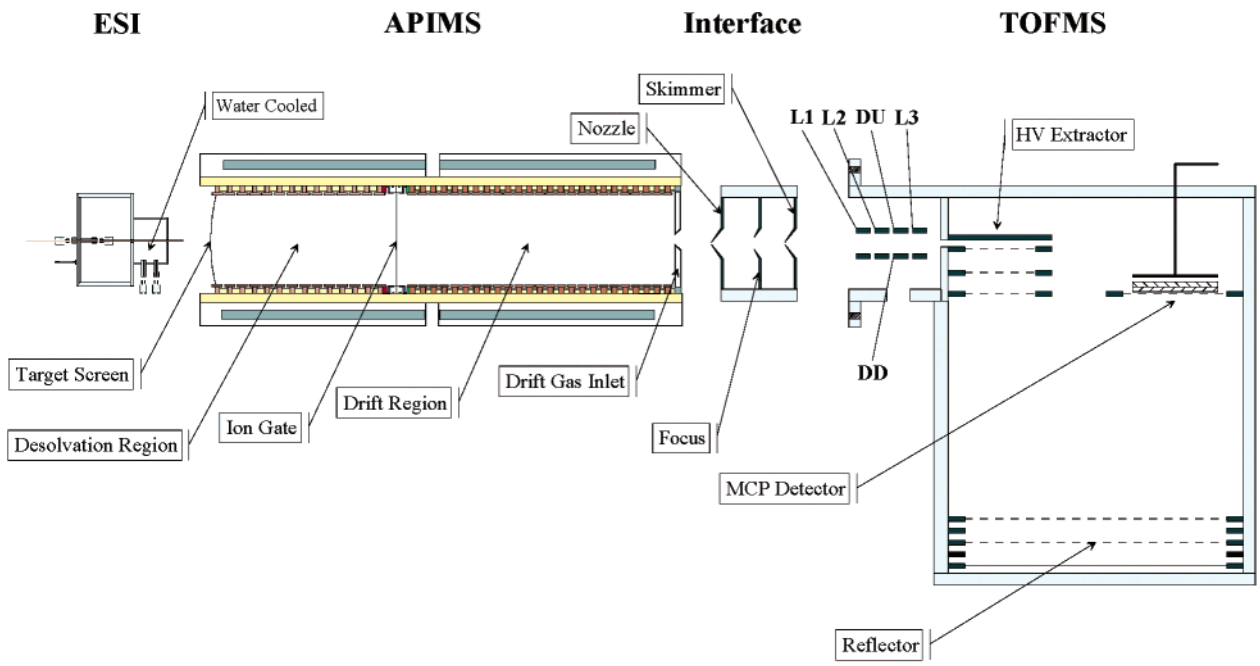

Figure 2. Side view schematic diagram of the electrospray ionization atmospheric pressure ion mobility orthogonal reflector time-of-flight mass spectrometer.

electric field, which facilitated separation based on differing analyte mobility constants. Ions exiting the APIMS drift tube entered a pressure interface where parent ions were then transported through a series of lenses into the TOFMS.

A continuous flow of solvent through the ESI source was provided by a KD Scientific (New Hope, PA) 210 syringe pump that maintained a solution flow rate of 7 μL/min for each run. All dissolved compound solutions were sprayed in the positive ion mode with a needle voltage of +3.5 KV with respect to the target screen of the APIMS. The basic stacked-ring design of the APIMS has been described, and modifications to the original design were reported.[20] The APIMS was divided into two regions, the desolvation (11 cm in length) and the drift (15 cm in length) regions. Ions were pulsed into the drift region by a Bradbury-Nielsen-style ion gate located between the two sections of the APIMS tube.[21] Both regions consisted of alternating high-purity alumina spacers (Haldenwanger, Berlin, Germany) and stainless steel rings. The conducting rings were connected via 500-kΩ and 1-MΩ high-temperature resistors (Caddock Electronics Inc., ±1%) for the desolvation and drift regions, respectively. A countercurrent flow of preheated nitrogen drift gas was introduced at the end of the drift region at a rate of 1 L/min. The temperature in both the drift and desolvation regions was maintained at 200 °C. Typical atmospheric pressures in Pullman, WA, where these experiments were conducted, ranged from 690 to 705 Torr. The applied electric field strength was held at 513 V/cm via a total drift voltage of +7.7 kV.

The APIMS was interfaced to a TOFMS through a pressure interface where ions exiting the drift region of the APIMS tube entered the mass spectrometer through a 300-μm pinhole nozzle (+200 V) and underwent a pressure drop from 690 to 705 to 1.5 Torr (600 L/min DS602 rotary vane pump, Varian, Walnut Creek, CA). A focusing lens in the interface allowed control of the collisional energy of the ions with residual gas particles. Thus, electrosprayed ions could be fragmented by collision-induced dissociations or pass through the pressure interface intact, depending on the potential applied to the focusing lens.[18] The ions exited the pressure interface through a second 300-μm skimmer cone which was operated at +100 V. Once through the second pinhole, the primary beam of ions entered the first differentially pumped region of the TOFMS held at $\sim 2 \times 10^{-4}$ Torr by a 46 L/s V70 turbo pump (Varian, Lexington, MA). A deflector and a series of lenses (labeled L1−L3, DU, and DD in Figure 2) were used to focus the ions into the main TOFMS chamber through a 2 mm × 10 mm slit. The TOFMS chamber was maintained at 4×10^{-6} Torr (250 L/s V250 turbo pump, both turbo pumps were backed by a 100 L/min DS102 rotary vane pump, Varian). Segments of the primary beam of ions were orthogonally extracted by a bipolar extractor pulsed at 20−80 kHz (Ionwerks pulser model HVPS, Houston, TX). The ions were then further accelerated into the −2000 V drift region followed by reflection and detection by a series microchannel plates (MCPs) with a chevron configuration. The operation and comprehensive description of the orthogonal reflector time-of-flight mass spectrometer may be found in ref 22.

Data acquisition for this experimental setup consisted of a timing sequence that was comprised of a real-time two-dimensional matrix of simultaneous mobility drift and mass flight times. Ions were typically gated for 0.15 ms into the drift region at a frequency of 50 Hz. This allowed for a maximum of 20 ms for the APIMS mobility data to be acquired. The TOFMS extraction frequency was set to 50 kHz, which provided a mass spectrum that consisted of ions with flight times up to 20 μs. Therefore, within each 20-

(19) Hill, H. H.; Siems, W. F.; Louis, R. H.; McMinn, D. G. *Anal. Chem.* **1990**, 62, 1201A. Helden, G. V.; Hsu, M. T.; Kemper, P. R.; Bowers, M. T. *J. Chem. Phys.* **1991**, *95*, 3835.

(20) Wu, C.; Siems, W. F.; Asbury, R. G.; Hill, H. H., Jr. *Anal. Chem.* **1998**, *70*, 4929−4938. Asbury, R. G.; Hill, H. H., Jr. *Microcolumn Sep.* **2000**, *12*, 391.

(21) Bradbury, N. E.; Neilson, R. A. *Phys. Rev.* **1936**, *49*, 388.

(22) Gonin, M.; Fuhrer, K.; Schultz, A. J. *12th Sanibel Conference on Mass Spectrometry*; Field Portable and Miniature Mass Spectrometry, 2000.

ms mobility time window, there were effectively 1000 TOF extractions. The APIMS ion gate and the TOFMS extractor were both triggered by a personal computer (PC)-based timing controller (Ionwerks model 307-001). Data acquisition could be delayed with respect to both, APIMS gate and TOFMS extraction, to reduce the size of the data array. Experimental data acquisitions were typically run for 15 min to provide clear ion statistics. This ensured that the effects of ionization efficiency and ion transmission were not a limiting factor when limits of detection were determined. Flight times were recorded by a time-to-digital converter (TDC, Ionwerks model TDCX4), activated by the same timing controller. Synchronization of this electronic hardware was facilitated by the use of a dual Pentium III workstation running Ionwerks two-dimensional acquisition software. Spectral compilations of data once acquired were then exported into both 2D Transform[23] and 3D NoeSYS[24] software for processing.

Calculations. The drift time, t_d, of an ion in the APIMS drift tube is defined as the time required for ions to travel through the length of the drift cell space, L, in centimeters, as given by

$$t_d = L^2/KV \quad (1)$$

where the mobility of the ions, K ($cm^2/(V\ s)$), is inversely proportional to the voltage, V, applied across the drift region. However, to take into account varying environmental and experimental conditions, it is practical to discuss ion drift times in terms of reduced mobility constants (K_o)[20] which are defined by

$$K_o = (L^2/Vt_d)(273.5/T)(P/760) \quad (2)$$

where L is the drift region length (15.0 cm), V is the drift voltage (7700 V), T is the effective temperature in the drift region (200 °C), and P is the pressure (695 Torr).

The flight time, τ_f, of an ion product refers to the time required for ions to traverse the length, l, from the high-voltage extractor to the microchannel detection plates in the TOFMS flight chamber as shown by

$$\tau_f = l(M/2E_{kin})^{1/2} \quad (3)$$

where M is the ion mass and E_{kin} is the kinetic energy of the ions. Theoretical limits of detection were also explored through the use of the following relationship:

$$DL_1(t_1)^{1/2} = DL_2(t_2)^{1/2} \quad (4)$$

where DL_1 and DL_2 are the experimental and theoretical detection limits, and t_1 and t_2 are the experimental and theoretical acquisition times, respectively. Moreover, to compensate for small fluctuations in instrumental operating condition a linear reference trend-line was employed:

$$t_s = mM + A \quad (5)$$

(23) Transform V3.4, Fortner Software LLC, Sterling, VA, 1998.
(24) NoeSYS V2.4, Research Systems Inc., Boulder, CO, 2000.

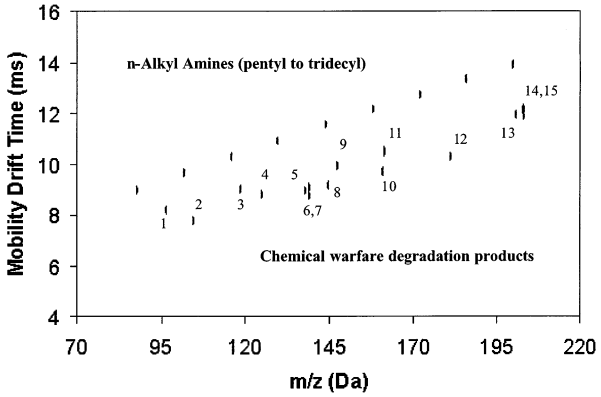

Figure 3. IMMS two-dimensional spectrum of CW (numbered) degradation products overlaid with a homologous reference series of *n*-alkylamines (not numbered) at 5 ppm. Ions from the CW degradation products were identified as follows: 1, methylphosphonic acid $(M + H)^+$; 2, thiodiglycol $(M + H - H_2O)^+$; 3, methylphosphonic acid $(M + Na)^+$; 4, ethylmethylphosphonic acid $(M + H)^+$; 5, thiodiglycol sulfoxide $(M + H)^+$; 6, isopropylmethylphosphonic acid $(M + H)^+$; 7, 1,4-dithiane $(M + H_2O + H)^+$; 8, thiodiglycol $(M + Na)^+$; 9, ethylmethylphosphonic acid $(M + Na)^+$; 10, thiodiglycol sulfoxide $(M + Na)^+$; 11, isopropylmethylphosphonic acid $(M + Na)^+$; 12, diisopropylmethylphosphonate $(M + H)^+$; 13, cyclohexylmethylphosphonic acid $(M + Na)^+$; 14, pinacolylmethylphosphonic acid $(M + Na)^+$; and 15, diisopropylmethylphosphonate $(M + Na)^+$. Ions from the *n*-alkylamines were identified as the $(M + H)^+$ products of pentyl-, hexyl-, heptyl-, octyl-, nonyl-, decyl-, undecyl-, dodecyl-, and tridecylamine.

where t_s, is the drift time of the standard, m is the slope, which is indicative to the ion density, and A is the intercept, which is correlated to the polarization of the ion-drift gas collision.

RESULTS AND DISCUSSION

Rapid Identification of CW Degradation Products. Standard CRM solutions for each of the CW degradation products were prepared and electrosprayed into the ESI/APIMS/TOFMS instrument. Figure 3 shows the two-dimensional (2-D) separation of a rapid acquisition of a solution (5 ppm) of all nine CW degradation products overlaid with a homologous series of *n*-alkylamines (described in next section). Both the protonated and sodium adduct forms of the CW degradation ion products were identified as follows: 1, methylphosphonic acid $(M + H)^+$; 2, thiodiglycol $(M + H - H_2O)^+$; 3, methylphosphonic acid $(M + Na)^+$; 4, ethylmethylphosphonic acid $(M + H)^+$; 5, thiodiglycol sulfoxide $(M + H)^+$; 6, isopropylmethylphosphonic acid $(M + H)^+$; 7, 1,4-dithiane $(M + H_2O + H)^+$; 8, thiodiglycol $(M + Na)^+$; 9, ethylmethylphosphonic acid $(M + Na)^+$; 10, thiodiglycol sulfoxide $(M + Na)^+$; 11, isopropylmethylphosphonic acid $(M + Na)^+$; 12, diisopropylmethylphosphonate $(M + H)^+$; 13, cyclohexylmethylphosphonic acid $(M + Na)^+$; 14, pinacolylmethylphosphonic acid $(M + Na)^+$; and 15, diisopropylmethylphosphonate $(M + Na)^+$, where the overall 2-D mobility/mass IMMS data for all of the CW degradation products were acquired at once. This made it possible to directly determine each of the ion products, mobility drift, and mass flight times produced from a single experimental run.

Although the rapid detection of these CW degradation products was achieved in a single ion mobility spectrum, it was essential not to overlook the importance of the combined 2-D mobility/mass mode of IMMS analysis and the additional separation power it provides for the resolution of more complex mixtures. This

Table 1. List of Masses, Ion Products, K_o Values, Experimental Limits of Detection, and Calculated Limits of Detection for Both Nerve and Vesicant CW Degradation Product CRMs

compound	mass	ion products	K_o (lit. K_o)[a]	LOD (ppb)[b] CC (r^2)[c] 15 min	TLOD (ppb)[d] 4 min	TLOD (ppb)[d] 60 min
1,4-dithiane	139	$(M + H_2O + H)^+$	1.72	51 (0.9978)	99	25
thiodiglycol	145	$(M + Na)^+$	1.68 (1.66)	nd[e]	nd	nd
	105	$(M + H - H_2O)^+$	1.93 (1.90)	20 (0.9560)	39	10
thiodiglycol sulfoxide	161	$(M + Na)^+$	1.59	45 (0.9987)	87	23
	139	$(M + H)^+$	1.77	18 (0.9992)	35	9
methylphosphonic acid	119	$(M + Na)^+$	1.71 (1.69)	nd	nd	nd
	97	$(M + H)^+$	1.82 (1.88)	560 (0.9981)	1084	280
ethylmethylphosphonic acid	147	$(M + Na)^+$	1.54 (1.54)	1700 (0.9834)	3292	850
	125	$(M + H)^+$	1.75 (1.78)	420 (0.9982)	813	210
isopropylmethylphosphonic acid	321	$(2M - H + 2Na)^+$	1.51	nd	nd	nd
	277	$(2M + H)^+$	1.21	nd	nd	nd
	161	$(M + Na)^+$	1.47	850 (0.9953)	1646	425
	139	$(M + H)^+$	1.72	1230 (0.9853)	2382	615
cyclohexylmethylphosphonic acid	201	$(M + Na)^+$	1.29	1500 (0.9972)	2905	750
pinacoylmethylphosphonic acid	203	$(M + Na)^+$	1.29 (1.27)	1310 (0.9951)	2536	655
diisopropylmethylphosphonate	383	$(2M + Na)^+$	0.961	nd	nd	nd
	361	$(2M + H)^+$	1.02	nd	nd	nd
	203	$(M + Na)^+$	1.30	10 (0.9980)	19	5
	181	$(M + H)^+$	1.50	700 (0.9932)	1355	350

[a] Literature K_o values.[17] [b] Limits of detection determined by the concentration producing a signal three times that of the noise. [c] Correlation coefficient calculated over 2 orders of magnitude using at least four data points. [d] Theoretical limits of detection via eq 4. [e] nd, not determined.

advantage was illustrated with the careful examination of the mobility/mass products found in the 2-D data set shown by Figure 3. In this example, it became apparently clear that a single mode of analysis was not capable of completely separating the mixture. The mobility spectrum alone resolved almost all of the CW degradation products with the exception to 3−8, 9, and 12−15, which all had relatively similar mobility drift times that overlapped in some cases. Similarly, the extracted mass spectrum alone could not clearly determine all CW degradation products. Products 6/7, 10/11, and 14/15 all had overlapping masses. However, the combination of these two modes of identification provided a very powerful means for the rapid, concise identification and quantification of these aqueous CW degradation products.

Trend-Line Reference Analysis. The identification of differing mobility/mass trends of ion products in large 2-D IMMS data sets has become valuable tool for the evaluation of these complex product spectra.[25] Clemmer et al. have used trend lines to distinguish between two spectrally complex data sets for low-mobility (singly charged) products as compared to that of higher mobility (doubly charged) peptide ions.[26] Russell et al. have employed the use of an internal standard for the purposes of reference, with the knowledge that a series of ions could be studied to produce mobility/mass trends that are distinguishable from one another.[27] In this work, external standards were used by electrospraying a homologous series of reference analytes that covered the dynamic range of the masses studied. These standards proved to be more useful in determining optimal instrumental operating conditions, as well as serving as a baseline reference point to which the experimental analytes of interest were compared.

The introduction and addition of a homologous series of *n*-alkylamines (pentyl-, hexyl-, heptyl-, octyl-, nonyl-, decyl-, undecyl-, dodecyl-, and tridecylamine) as external standards produced a "trend line" to which the CW degradation products were referenced; their IMMS spectrum is shown in Figure 3. These *n*-alkylamines formed a linear reference trend line where the reference slope (m_r) and intercept (A_r) were 0.0438 and 5.13, respectively. In comparison, the CW degradation products slope (m_{cw}) and intercept (A_{cw}) of all nine CW degradation products grouped as a single trend line were respectively 0.0364 and 4.24. This gave an overall ΔM of 0.0074 and ΔA of 0.89 for these experimental operating conditions, where ΔM and ΔA are respectively defined as the difference between $m_r - m_{cw}$ and $A_r - A_{cw}$. Under nonstandard or field conditions, deviations in values of ΔM and ΔA can be assessed for changes in environmental conditions such as temperature, pressure, humidity, drift gas selections, and impurities within the drift gas. A reference trend line can serve as a way to improve the accuracy of the mobility measurement by providing a mobility reference point at each mass along the trend-line axis.

Note that the *n*-alkylamine trend line occurred at mobility drift times greater than that of the CW degradation products. For the same molecular weight, *n*-alkylamines are physically larger in size than the CW degradation products. In fact, *n*-alkylamines were chosen as the trend-line reference because they are straight-chain amines. Amine compounds in general respond strongly to ESI, and straight-chain ions produce the largest ions possible for a given molecular weight. Thus, the reference trend line will not interfere with the more dense product ions of the CW degradation products, yet provide a convenient reference point for mobility

(25) Valentine, S. J.; Kulchania, M.; Srebalus Barnes, C. A.; Clemmer, D. E. *Int. J. Mass Spectrom.* **2001**, *212* (1−3), 97−109.
(26) Srebalus Barnes, C. A.; Hilderbrand, A. E.; Valentine, S. J.; Clemmer, D. E. *Anal. Chem.* **2002**, *74*, 26−36.
(27) Woods, A. S.; Koomen, J. M.; Ruotolo, B. T.; Gilling, Russel, D. H.; K. J.; Fuhrer, K.; Gonin, M.; Egan, T. F.; Schultz, J. A. *J. Am. Soc. Mass Spectrom.* **2002**, *13*, 166−169.
(28) Karpas, Z. *Anal. Chem.* **1989**, *61*, 684. Karpas, Z.; Berant, Z.; Shahal, O. *J. Am. Chem. Soc.* **1989**, *111*, 6015. Berant, Z.; Karpas, Z.; Shahal, O. *J. Phys. Chem.* **1989**, *93*, 7534.

Table 2. List of Mass, Products, and K_o Values for a Homologous Set of *n*-Alkylamines

compound	mass	products	K_o (lit. K_o)[a]
pentylamine	88	$(M + H)^+$	1.72 (1.72)
hexylamine	102	$(M + H)^+$	1.60 (1.61)
heptylamine	116	$(M + H)^+$	1.50 (1.50)
octylamine	130	$(M + H)^+$	1.41 (1.42)
nonylamine	144	$(M + H)^+$	1.34 (1.35)
decylamine	158	$(M + H)^+$	1.28 (1.28)
undecylamine	172	$(M + H)^+$	1.22 (1.23)
dodecylamine	186	$(M + H)^+$	1.16
tridecylamine	200	$(M + H)^+$	1.11

[a] Literature K_o values.[28]

throughout the mass range of interest. By using a homologous series of analytes in this manner, a baseline reference trend line could then be used as a fourth mode (size-to-charge drift times, mass-to-charge flight times, peak intensity, and "trend-line normalization") of compound identification integrity.

Products, Dynamic Ranges, Limits of Detection, and Correlation Coefficients. Tabulated values for each of the products that were experimentally analyzed are shown in Table 1. Here the masses (M), ion products $(M + N)^n$, reduced mobility constants (K_o), and limits of detection (LODs) for 15 min of analysis and theoretical limits of detection (TLODs) for 4- and 60-min sample runs for both nerve and vesicant CW degradation product CRMs are examined. While most compounds produced both protonated ions, $(M + H)^+$, and prominent development of sodium ion adducts, $(M + Na)^+$, some products formed adducts that deviated from this trend; 1,4-dithiane produced a protonated ion with addition of a water molecule, $(M + H_2O + H)^+$. The extent of sodium adduct formation was such that two compounds, cyclohexyl- and pinacoylmethylphosphonic acids, produced only peaks associated with sodium. An additional deviation from the primary trend was the ion formed by the compound containing thiodiglycol. The alcohol group associated with this product was believed to play a significant role in the formation of the ion that corresponded to the loss of a water molecule $(M - H_2O + H)^+$. Dimer formation was also observed in some cases with isopropylmethylphosphonic acid and diisopropylmethylphosphonate, which produced $(2M + H)^+$, $(2M - H + 2Na)^+$, and $(2M + Na)^+$ products. Each of these products and the corresponding experimental conditions that produced these products will be addressed in the next section. Comparison of these experimentally determined K_o values with those found in the current literature indicated that this IMMS instrument provided an accurate method of detection and identification of CW degradation products.[17] Last, Table 2 provides the K_o values for the protonated form of the homologous series of *n*-alkylamines. These compounds formed the reference trend line that increased by 14 m/z units and 0.6 mobility unit for each compound.

The dynamic range for diisopropylmethylphosphonate was determined to be 4 orders of magnitude, ranging from 10 ppb to 100 ppm as shown in Figure 4A. Data from the analysis of all of the CW degradation products examined in this study produced similar graphs and dynamic ranges. Each compound was analyzed for 15 min in triplicate with a series of standards ranging from 100 ppb to 100 ppm. Figure 4B shows the linear portion of Figure 4A. This graph demonstrates the linear response produced by the instrument (correlation coefficient >0.99) for diisopropylmethylphosphonate in the range 10−2500 ppb or 2 orders of magnitude. This is a typical linear range for ESI sources and for most ionization sources used with IMS systems. From this calibration curve, the LOD was determined to be 10 ppb for diisopropylmethylphosphonate using the standard definition of S/N > 3. Again similar calibration curves were made for each compound where the LODs and correlation coefficients were determined. The TLOD for each compound was calculated, according to eq 4, for acquisition times of 4 and 60 min. More important was the finding that each TLOD value reported was within a 95% confidence level. These results are summarized in the last three columns of Table 1. LODs were excellent for the sulfur-containing vesicant CW degradation products (~30 ppb) but somewhat poorer for the phosphonic acids derived from the CW nerve agents (~1000 ppb). As these compounds are fairly strong acids (~2.54 pK_a), it is expected that signal intensity for positive ion mode would be negligible. Overall detection limits ranged from low ppb

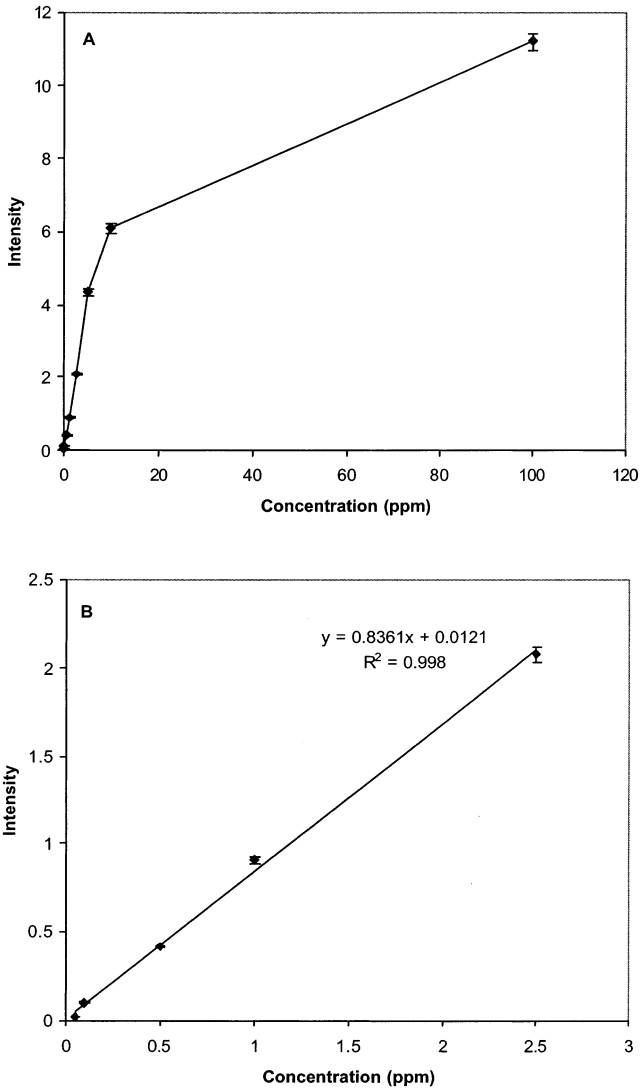

Figure 4. (A) Dynamic range curve for diisopropylmethylphosphonate. The dynamic range was from ~10 ppb to 100 ppm or 4 orders of magnitude. (B) Calibration curve for diisopropylmethylphosphonate in the range of 10−2500 ppb. The error bars for some of the data points are contained within the point itself.

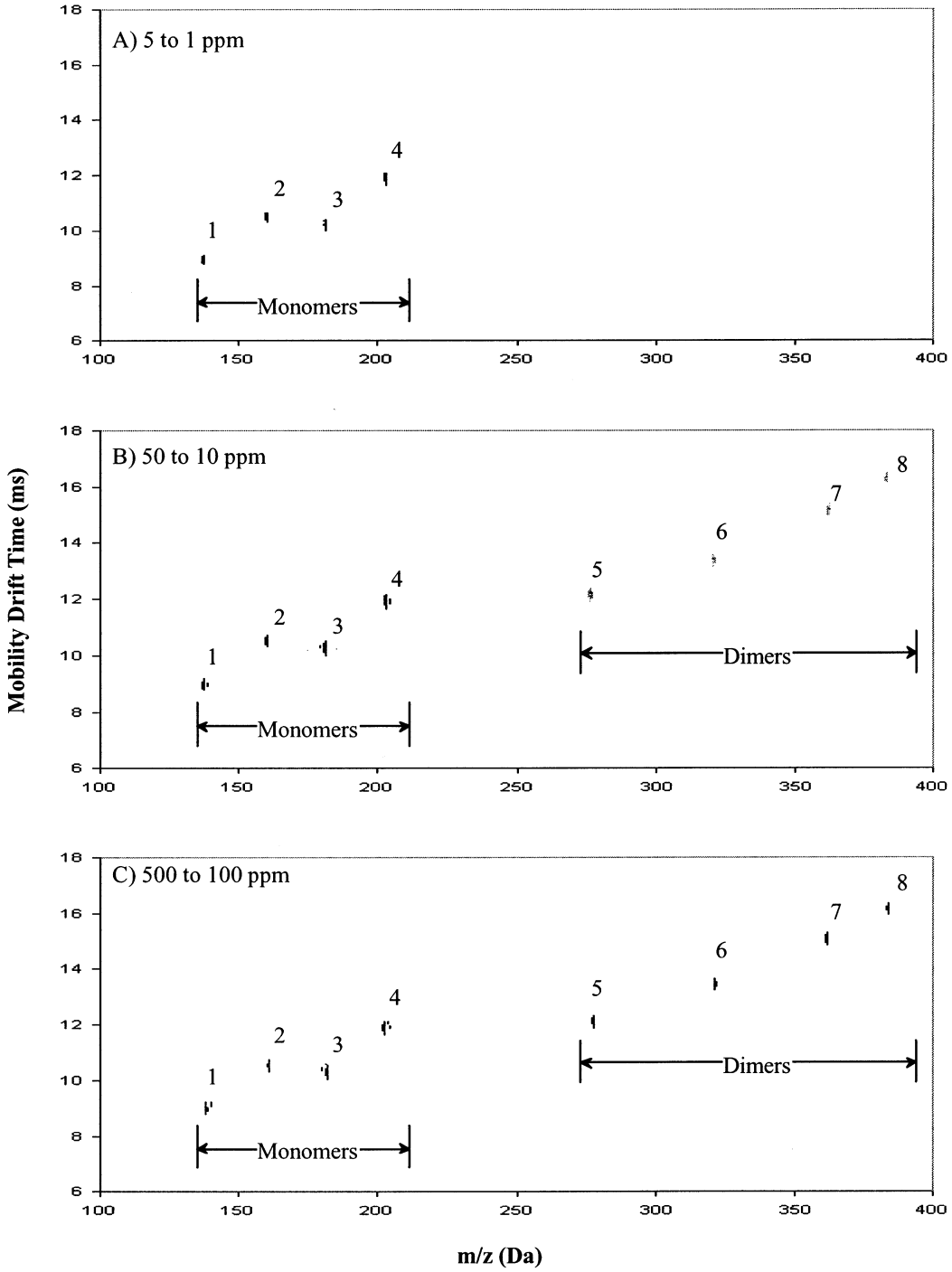

Figure 5. IMMS spectra of dimer formation with a mixture of isopropylmethylphosphonic acid and diisopropylmethylphosphonate at concentration ratios of (A) 5−1, (B) 50−10, and (C) 500−100 ppm, respectively. Peaks are identified as follows: 1, isopropylmethylphosphonic acid $(M + H)^+$; 2, isopropylmethylphosphonic acid $(M + Na)^+$; 3, diisopropylmethylphosphonate $(M + H)^+$; 4, diisopropylmethylphosphonate $(M + Na)^+$; 5, isopropylmethylphosphonic acid $(2M + H)^+$; 6, isopropylmethylphosphonic acid $(2M - H + 2Na)^+$; 7, diisopropylmethylphosphonate $(2M + H)^+$; 8, diisopropylmethylphosphonate $(2M + Na)^+$.

to low ppm with the poorer detection limits coming from the electronegative phosphonic acids.

Dimer Formation of Phosphonic Acid Mixtures at High Concentrations. When the dynamic range for the phosphonic acids was determined in the positive mode, it was noted that at concentrations at or above 10 ppm the slope of the calibration curve flattened out, as seen in Figure 4A. In these experiments, the formation of dimer peaks at longer drift and flight times was also seen, indicating the occurrence of ion clustering. Figure 5 shows a 2-D spectrum for the mixture of isopropylmethylphosphonic acid and diisopropylmethylphosphonate where the corresponding monomer and dimer products were identified as follows: 1, isopropylmethylphosphonic acid $(M + H)^+$; 2, isopropylmethylphosphonic acid $(M + Na)^+$; 3, diisopropylmethylphosphonate $(M + H)^+$; 4, diisopropylmethylphosphonate $(M + Na)^+$; 5, isopropylmethylphosphonic acid $(2M + H)^+$; 6, isopropylmethylphosphonic acid $(2M - H + 2Na)^+$; 7, diisopropylmethylphosphonate $(2M + H)^+$; 8, diisopropylmethylphosphonate $(2M + Na)^+$.

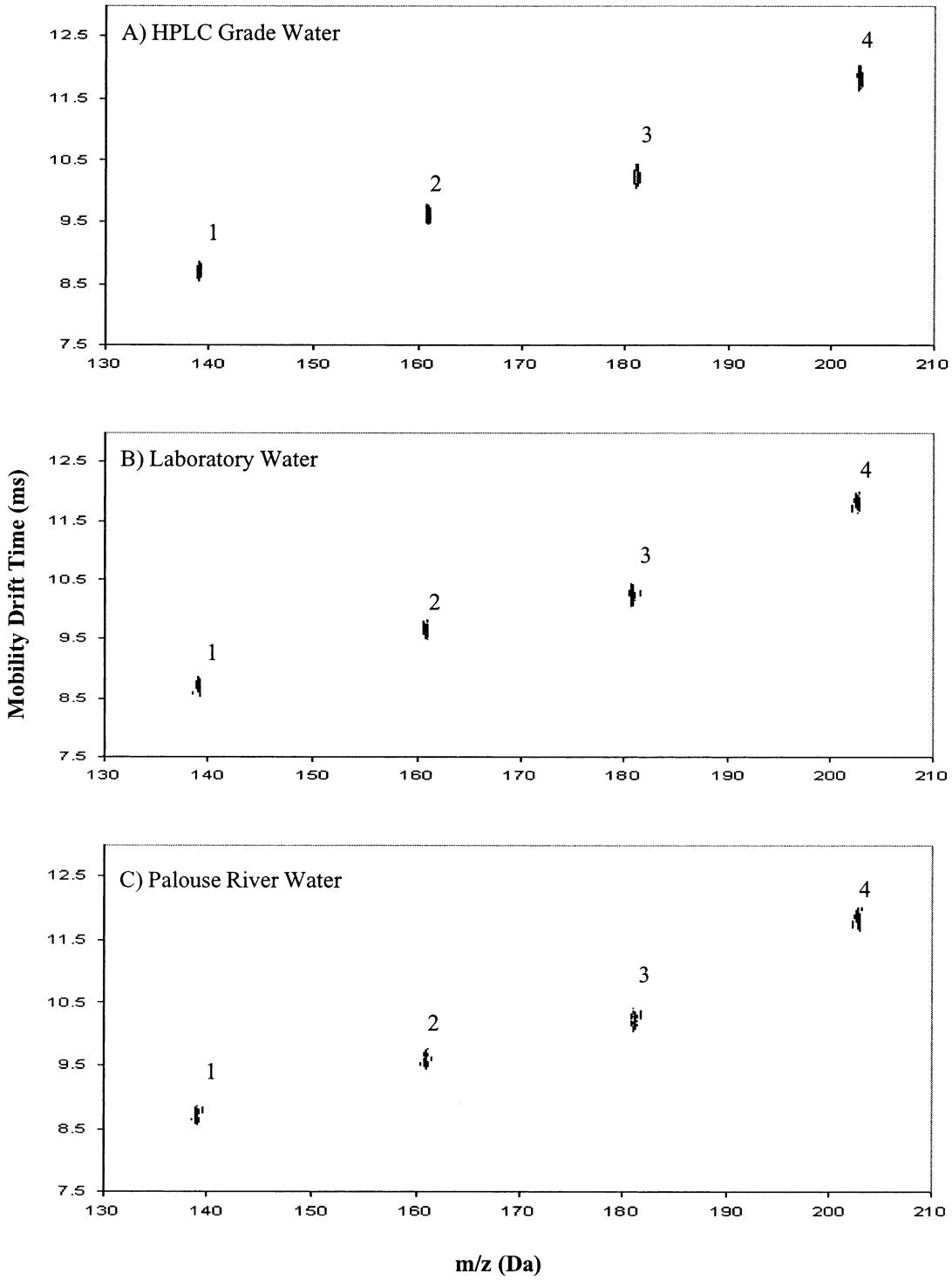

Figure 6. IMMS spectra of 1 ppm CW degradation products in different water sample matrixes: (A) 47.5% methanol, 47.5% HPLC grade water, and 5% acetic acid; (B) 47.5% methanol, 47.5% laboratory water, and 5% acetic acid; and (C) 47.5% methanol, 47.5% Palouse River water, and 5% acetic acid. Peaks are identified as follows: 1, thiodiglycol sulfoxide $(M + H)^+$; 2, thiodiglycol sulfoxide $(M + Na)^+$; 3, diisopropylmethylphosphonate $(M + H)^+$; and 4, diisopropylmethylphosphonate $(M + Na)^+$.

A noted exception to the common trend of product formation was seen when one isopropylmethylphosphonic acid exchanged a proton from an alcohol functional group with a sodium to yield a $(2M - H + 2Na)^+$ dimer.

Figure 5A illustrates spectra obtained at a concentration of 5 and 1 ppm for isopropylmethylphosphonic acid and diisopropylmethylphosphonate, respectively. At this concentration both the $(M + H)^+$ and $(M + Na)^+$ ions are observed with no indication of dimer formation previously seen at elevated drift and mass flight times. At these lower concentrations, each phosphonic acid produced two ionic products where quantification would be possible. Figure 5B shows a mixture of the same two compounds with concentrations of 50 and 10 ppm, respectively. In this case, the formation of dimer products for both analytes was beginning

to be observed. The extent of the dimer formation ($(2M + H)^+$, $(2M + NA)^+$, and $(2M - H + 2Na)^+$) were not large in relation to the intensity associated with the monomers, but quantification of monomers at this concentration could lead to false calculated concentrations of lower values than are present. Figure 5C shows the spectra of the same two phosphonic acids at concentrations of 500 and 100 ppm, respectively. In this case, significant ion dimer formation at elevated mobilities and mass flight times was observed. Examination of theses data indicated that the dimer ions were either formed at the ion source and not in the pressure interface or the TOFMS. If dimers had formed post APIMS, the dimer products would have had the same mobilities as the monomers, which was not the case in this study.

Analysis of CW Degradation Products in Natural Water Samples. The ability of IMMS to determine nerve and vesicant CW degradation products from actual environmental samples was investigated. HPLC grade water, laboratory water, and Palouse River water was used because of its accessibility. The Palouse River water was collected directly from a flowing portion of the river. Again, the only sample pretreatment for these water samples was filtering with a 0.20-μm filter in order to avoid particulate matter from plugging the ESI needle. All water samples were spiked with diisopropylmethylphosphonate and thiodiglycol sulfoxide CW degradation products at concentrations of 10 ppm. After the spiked solution was diluted with methanol and acetic acid to produce the standard ESI solvent ratios (47.5% methanol, 47.5% water, 5% acetic acid), the resulting CW degradation product concentrations were 1 ppm.

The results for HPLC grade water were shown in Figure 6A, where the products were as follows: 1, thiodiglycol sulfoxide $(M + H)^+$; 2, thiodiglycol sulfoxide $(M + Na)^+$; 3, diisopropylmethylphosphonate $(M + H)^+$; and 4, diisopropylmethylphosphonate $(M + Na)^+$. Figure 6B showed the spectra for the laboratory water spiked solution. In this case, the shapes were very similar compared to that of the HPLC grade water sample. Figure 6C showed the analytical results of the spiked Palouse River water sample. It is important to notice that, at the 1 ppm level, no interferences in the real sample were observed. More importantly, the four test CW degradation products used in this study were easily detected at this level. These results of spiked water samples demonstrated the ability of the IMMS to rapidly analyze a real sample for CW degradation agents in less than 1 min, without any significant sample cleanup.

CONCLUSIONS

IMMS shows the potential to be a very rapid and sensitive analytical method for the identification and quantification of Schedule 1, 2, or 3 toxic chemicals or precursor for CWC treaty verification and related compounds. The instrumental analysis time is short—less than 1 min—with good sensitivity where the limits of detection are less than 100 ppb for most compounds tested. For many cases, IMMS can replace slower chromatographic separation methods, thereby increasing sample throughput. Analysis of experimental K_o and literature K_o' values shows that instrumental reproducibility is excellent and that IMMS is capable of providing mobility data that can be matched to that obtained with other laboratory instruments. In addition, a homogeneous mixture of *n*-alkylamines can be used as a standard to produce a reference "trend line" for correcting variations in instrumental parametric fluctuations— such as pressure or temperature—during routine or field analysis. From these initial investigations, it appears feasible to use IMMS as a rapid screening method for CW-related compounds dissolved in aqueous environments for the purposes of treaty verification and ensuring the integrity of aqueous resources that are relied upon by both military and civilian populations. Perhaps even more important than the determination of CW-related compounds, IMMS may be applicable to most polar water-soluble organic compounds such as amines, phenols, acids, etc., that can be screened with IMMS.

ACKNOWLEDGMENT

The authors acknowledge Ionwerks Inc. of Houston, TX, for continued scientific correspondence. This work was supported in part by the United States Army Research Office (Grants DAAG559810107 and DAAD190010028).

Received for review April 7, 2002. Accepted June 18, 2002.

AC025687F